ELSEVIER

Ceramics International 30 (2004) 1301–1306

CERAMICS
INTERNATIONAL

www.elsevier.com/locate/ceramint

The electrical properties of Mn_3O_4-doped ZnO

Y.W. Hong, J.H. Kim*

Department of Inorganic Materials Engineering, Kyungpook National University, 1370 Sankyuk-Dong, Buk-Gu, Daegu 702-701, South Korea

Received 28 November 2003; received in revised form 18 December 2003; accepted 22 December 2003

Abstract

Polycrystalline ZnO doped with 1/3 mol% Mn_3O_4 was prepared by the conventional ceramic processing. From *J–E* characteristics the varistor behavior with nonlinear coefficient, α between 6 and 17 was confirmed in the Mn-doped ZnO sintered at 1000–1300 °C for 1 h in air, but was changed to ohmic behavior in the 1400 °C sintered specimen. In relation to the grain boundary resistivity, three activation energies of 0.37, 0.87 and 0.96 eV were detected from pre-breakdown *J–E–T* characteristic curves. The barrier height and donor concentration of the Mn-doped ZnO were calculated as about 1.0 V and $2 \times 10^{17}\ \mathrm{cm}^{-3}$ from *C–V* characteristics, respectively. Similar to commercial ZnO varistors, the deep bulk trap levels in Mn-doped ZnO were estimated as 0.13 and 0.25–0.32 eV by admittance spectroscopy. The varistor behavior of Mn-doped ZnO ceramics supports the formation of double Schottky type barrier in the grain boundary region. It is thought that the release and adsorption of oxygen on ZnO grain boundaries during the redox reaction of Mn ion is responsible for the varistor behavior of Mn-doped ZnO.

Keywords: C. Electrical properties; D. ZnO; E. Varistors; Manganese oxide

1. Introduction

Polycrystalline ZnO has numerous applications in such diverse areas as facial powders, piezoelectric transducers, varistors, phosphors, and transparent conducting films [1,2]. It is important to evaluate the defect levels in bulk ZnO especially in the application of ZnO varistors [2]. The deep or shallow trap levels commonly found in bulk ZnO are as interstitial zinc, oxygen vacancy, and impurity induced donor or acceptor levels [1–3]. It is known that the manganese oxide in ZnO varistors drastically improve the nonlinear *J–E* characteristics [1]. The equilibrium between di- and trivalent manganese oxides in oxygen atmosphere is expressed by the equation [5]:

$$4Mn_3O_4 + O_2 \xrightarrow{537\,^\circ C} 6Mn_2O_3 \xrightarrow{959\,^\circ C} 4Mn_3O_4 + O_2 \qquad (1)$$

Mn_3O_4 doping on ZnO is expected to cause interesting phenomena in relation to the point defect formation in polycrystalline ZnO. In this study, we prepared ZnO doped with 1/3 mol% Mn_3O_4 sintered at 1000–1400 °C and measured its *J–E–T*, *C–V* and *G–ω–T* characteristics. The origin of varistor behavior has been discussed in relation to interfacial and bulk traps.

2. Experimental procedure

Reagent grade ZnO (99.9%) and Mn_3O_4 (>99.0%) powders were used as sintering materials. ZnO admixed with 1/3 mol% Mn_3O_4 was prepared by ball milling in a polyethylene jar with zirconia balls of 5 mm diameter as milling media in ethanol. The slurry was dried into a cake, and was sieved through a 100 mesh screen to produce granules without binder. Granules were uniaxially pressed into pellets under 20 MPa and then CIPed at 98 MPa. The pellets were placed in an alumina crucible and sintered between 1000 and 1400 °C for 1hr in air at heating and cooling rates of 5 °C/min. Sintered pellets were trimmed into disks of 1.0 mm thick and 8.0 mm in diameter, and silvered on both sides for the electrical measurements. Commercial Ag-paste was used in the electroding, in which the disks were heat-treated at 600 °C for 10 min in air.

The dc current–voltage (*J–E*) characteristics were measured at 20 K increments between 300 and 500 K in air using a high voltage unit (Keithley 237).

In the breakdown region of *J–E* curve, the nonlinear coefficient (α) was obtained by the following empirical relation:

---

* Corresponding author. Tel.: +82-53-950-5637; fax: +82-53-950-5645.
E-mail address: jihkim@knu.ac.kr (J.H. Kim).

0272-8842/$30.00 © 2004 Elsevier Ltd and Techna Group S.r.l. All rights reserved.
doi:10.1016/j.ceramint.2003.12.028

$$J = CE^{\alpha}; \quad \alpha = \frac{\log(J_2/J_1)}{\log(E_2/E_1)} \tag{2}$$

where E_1 and E_2 are electric field corresponding to $J_1 = 1\,\mathrm{mA/cm^2}$ and $J_2 = 10\,\mathrm{mA/cm^2}$, respectively.

The breakdown field (E_b) and the leakage current density (J_L) were defined as the electric field at the current density of 1.0 mA/cm^2 and the current density for an electric field of 0.8 E_b, respectively.

Grain boundary resistivity, ρ, was determined from the slope of the pre-breakdown *J–E* curve, and plotted using $\ln\rho-(1/T)$ Arrhenius relation shown below to estimate the activation energy E_a [4].

$$\ln\rho = \ln\rho_0 + \left(\frac{E_a}{k}\right)\frac{1}{T} \tag{3}$$

Capacitance–voltage measurements were conducted at room temperature using an impedance/gain phase analyzer (HP 4194A) at 10 kHz. Obtained data were plotted according to the modified *C* versus *V* relation [6]:

$$\left(\frac{1}{C} - \frac{1}{2C_0}\right)^2 = \frac{2(\phi + V)}{e\varepsilon N_d} \tag{4}$$

where e is the electron charge, ε the permittivity of ZnO ($8.5\varepsilon_0$, ε_0 is the permittivity of vacuum), N_d the donor density, ϕ the barrier height, C and V are the capacitance and the applied voltage per grain boundary. Both N_d and ϕ were calculated from the slope and the intercept of $(1/C-1/2C_0)^2$ versus V plot. With these values, the depletion layer width (W) and the density of the interface states (N_t) have been estimated using the following equation:

$$W = \left(\frac{2\varepsilon\phi}{e^2N_d}\right)^{1/2}, \quad N_t = \left(\frac{2N_d\varepsilon\phi}{e}\right)^{1/2} \tag{5}$$

The admittance spectroscopy measurements for identifying deep bulk trap were carried out using an impedance/gain phase analyzer at frequencies ranging from 1.0 to 5.0 MHz with seven sampling points. In the examination of temperature response, the specimens were placed in a sample holder inside a furnace, and the admittance was measured between 77 and 400 K at a cooling rate of 1.0 °C/min with a computer-aided data acquisition system.

3. Result and discussion

The room temperature *J–E* characteristics of Mn-doped ZnO are shown in Fig. 1. All specimens except 1400 °C sintered one show clearly nonlinear *J–E* characteristics: α of 6.0–17.5; J_L of 0.1–0.4 mA/cm^2; ρ of 2.5×10^6 to $2.5 \times 10^9\ \Omega$ cm. Fig. 2 shows *J–E–T* characteristics at 300–500 K of Mn-doped ZnO sintered at 1000 °C. The inflection of the curves in the pre-breakdown region appeared above 400 K, which divided the curve into two regions of different slopes (A and B in Fig. 2). From the respective slope of the curve, grain boundary resistivity, ρ was obtained as a function of temperature.

Fig. 3 shows $\ln\rho-(1/T)$ relation obtained from Fig. 2, and Table 1 summarizes the varistor characteristics of Mn-doped ZnO, sintered between 1000 and 1400 °C. The specimens sintered below 1300 °C revealed single E_a of $\sim$0.4 eV at $T <$ 400 K. At $T = 400$ K, on the contrary, two distinct activation energies of 0.79–0.87 eV and 0.88–0.96 eV appeared based on the slopes A and B as shown in Fig. 2, respectively. The specimens sintered at 1300 and 1400 °C, however, revealed single E_a of 0.71 and 0.09 eV throughout the measuring temperature range of 300–500 K, respectively.

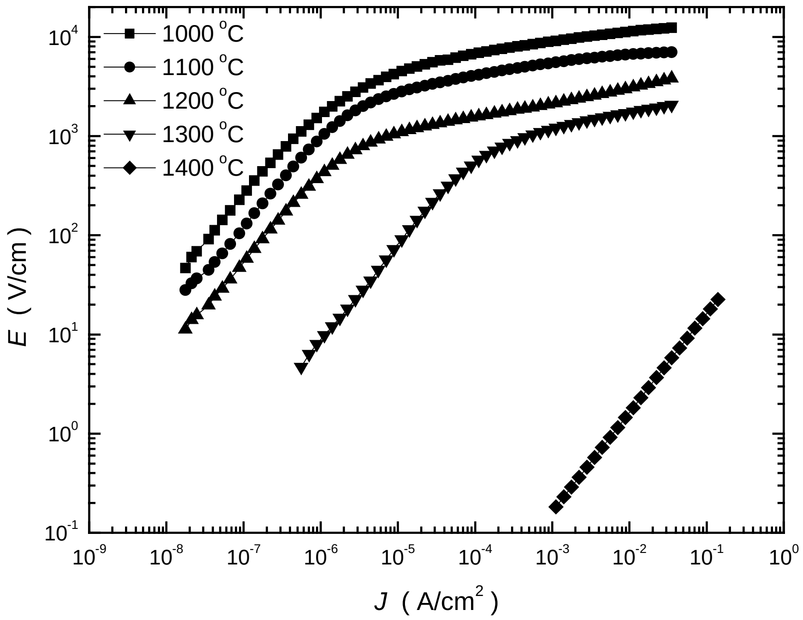

Fig. 1. *J–E* characteristics of Mn-doped ZnO (1/3 mol% Mn_3O_4) sintered at various temperatures for 1 h.

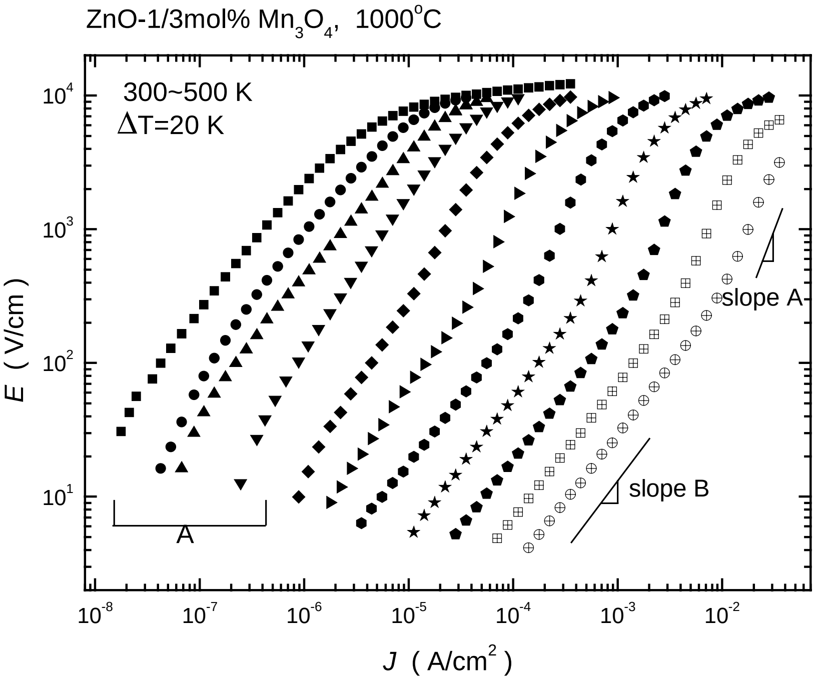

Fig. 2. Temperature dependence of J–E characteristics of Mn-doped ZnO sintered at 1000 °C, measured between 300 and 500 K at 20 K increments.

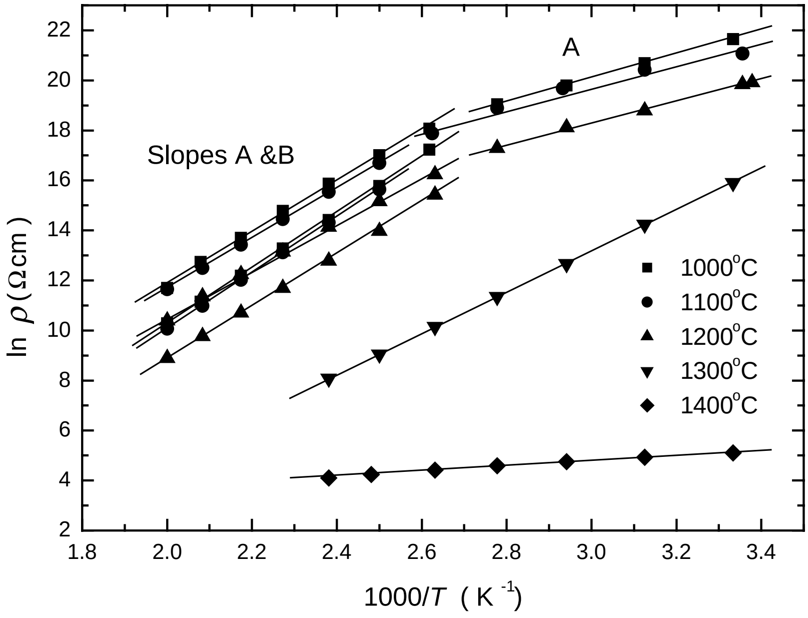

Fig. 3. Arrhenius plots of ln $\rho(T)$ vs. 1000/T for Mn-doped ZnO sintered at various temperatures.

Table 1
Summary of J–E characteristics of Mn-doped ZnO sintered at various temperatures

Sintering temperature (°C)	α	J_L (mA/cm^2)	E_b (V/cm)	ρ_{gb} (Ωcm)	E_a (eV)		
					A	Slope A	Slope B
1000	15.6	0.16	9030	2.48×10^9	0.40	0.86	0.96
1100	17.5	0.19	5480	1.11×10^9	0.37	0.87	0.96
1200	7.0	0.34	2120	0.41×10^9	0.37	0.79	0.88
1300	6.0	0.40	1183	2.46×10^6	–		0.71
1400	1.0	–	–	143	–		0.09

α: non-linear coefficient, J_L: leakage current density, E_b: breakdown field, ρ_{gb}: grain boundary resistivity at room temperature, E_a: activation energy.

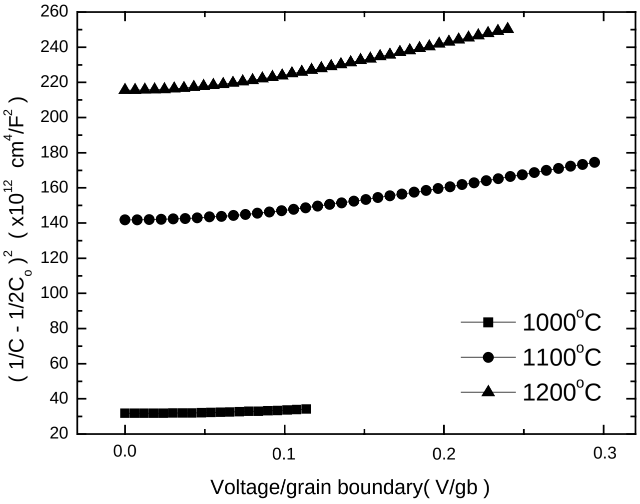

Fig. 4. *C–V* characteristics of 1/3 mol% Mn_3O_4-doped ZnO samples with sintering temperature.

It seems that the activation energy of pre-breakdown condition decrease with increasing sintering temperature of Mn-doped ZnO.

Fig. 4 shows *C–V* characteristics of Mn-doped ZnO, and N_d, N_t and ϕ_b calculated from the plot with increasing sintering temperature 1000 and 1200 °C, are summarized in Table 2. Both N_d and N_t decreased from 4.75 to 0.89 [$\times 10^{17}$ cm^{-3}] and 2.09 to 0.95 [$\times 10^{12}$ cm^{-2}], respectively, and W increased from 44 to 108 [nm]. The potential barrier height, ϕ was kept constant at ~1 eV in all the specimens. Consequently we conclude that the interfaces of Mn-doped ZnO grains form the double Schottky barrier and show the varistor behaviors.

The zero bias admittance (G) of Mn-doped ZnO at 1 MHz is plotted as a function of temperature in Fig. 5. The curves show two maxima apart in the temperature range. From these curves, peak temperatures (T_p) at admittance maxima have been determined as a function of frequency. According to Greuter and Blatter [1], the deep bulk trap states introduce screening charge into double Schottky barrier and result in a dispersion and singular broadness in zero bias admittance. The characteristic relaxation time, τ_n, for a deep bulk trap is given by [1]:

$$\tau_n = \frac{e}{2A^* \times T^2 g\sigma_n} \exp\left(\frac{E_{bt}}{kT}\right) \qquad (6)$$

where e is the electron charge, A^* the effective Richardson's constant (~30 A cm^{-2} K^{-2} for ZnO), T the temperature, g (1/2) the inverse of the degeneracy of the trap state, σ_n the capture cross section, E_{bt} the deep bulk trap below the conduction band edge, and k the Boltzmann constant.

Table 2
Summary of *C–V* characteristics of Mn-doped ZnO samples

Sintering temperature (°C)	N_d ($\times 10^{17}$ cm^{-3})	N_t ($\times 10^{12}$ cm^{-2})	ϕ_b (V)	W (nm)
1000	4.75	2.09	0.98	44
1100	1.16	1.00	0.91	86
1200	0.89	0.95	1.09	108

N_d and N_t: donor and interface trap densities, ϕ: potential barrier height, W: width of depletion layer.

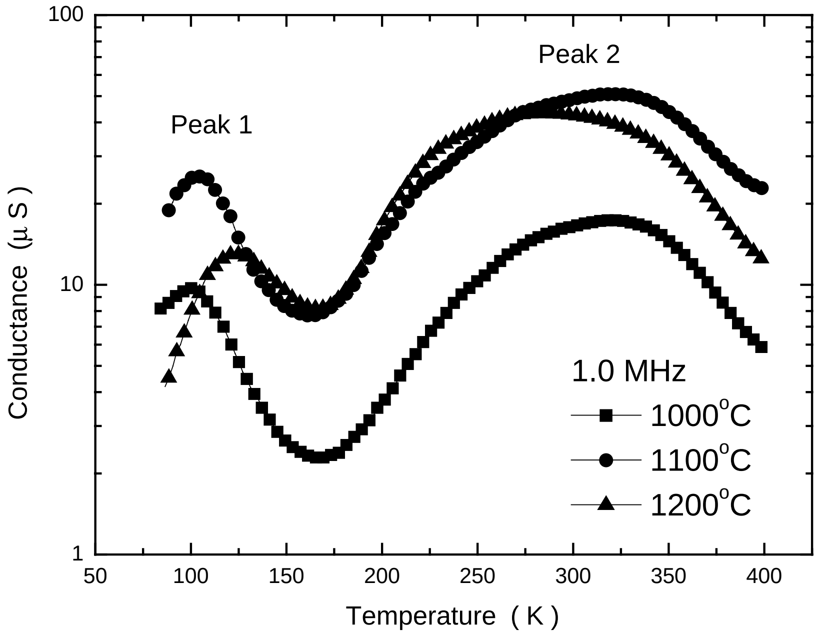

Fig. 5. Conductance as a function of temperature for Mn-doped ZnO sintered at 1000–1200 °C for 1 h, measured at 1.0 MHz.

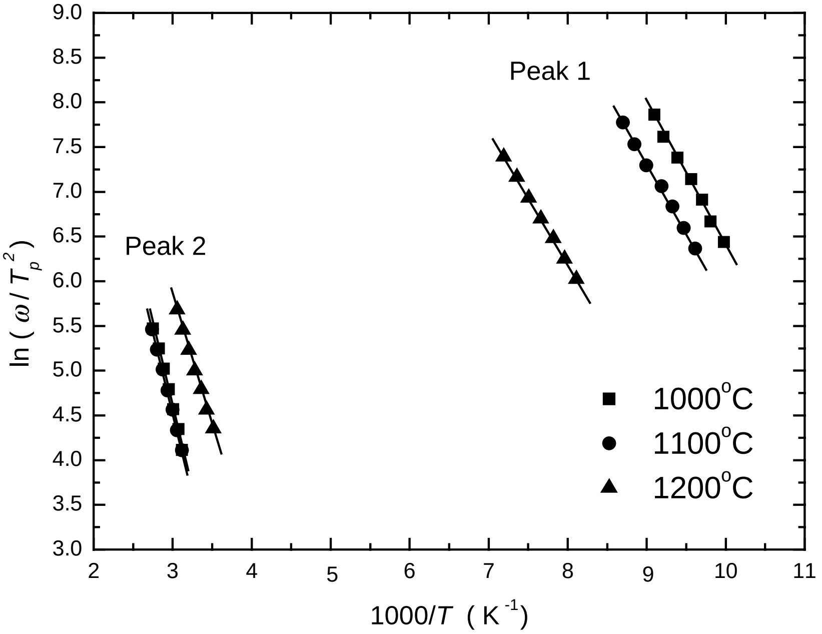

Fig. 6. Arrhenius plots of $\ln(\omega/T_p^2)$ vs. $1000/T$ for Mn-doped ZnO sintered at various temperatures.

Table 3
Calculated parameters from the Arrhenius plots shown in Fig. 6

Sintering temperature (°C)	Peak 1		Peak 2	
	E_1 (eV)	σ_1 ($\times 10^{-12}$ cm^2)	E_2 (eV)	σ_2 ($\times 10^{-14}$ cm^2)
1000	0.14	27.1	0.32	3.1
1100	0.13	6.6	0.31	2.2
1200	0.13	0.4	0.25	1.2

The deep bulk trap resonance occurs when $\omega\tau_n = 1$, that is, at a local maximum of the conductance G versus ω plot with temperature. The activation energies for the deep bulk trap levels in Eq. (6) can be obtained from the slope of the Arrhenius plot of $\ln(\omega/T_p^2)$ versus $1/T$, and the intercept is proportional to its capture cross section, σ_n. The $\ln(\omega/T_p^2)$ versus $1/T$ plot of Mn-doped ZnO is shown in Fig. 6, and the values of E_{bt} and σ_n for each samples determined from the slopes of the curves are listed in Table 3.

Two deep bulk traps of ~0.13 and ~0.3 eV are revealed by $\ln(\omega/T_p^2)$ versus $1/T$ plot of Mn-doped ZnO below 400 K. The 0.13 eV trap level has a large capture cross section distributed from 2.7×10^{-11} to 4.0×10^{-13} cm^2. The trap level of 0.13 eV is thought to stem from the attractive coulombic center [1]. The trap levels of 0.25–0.32 eV with capture cross section of 10^{-14} cm^2 order can be assigned to singly charged oxygen vacancy, $V_O^\bullet$, which is commonly accepted in ZnO varistors. The presumed level gradually decreased with sintering temperature. As further splitting of the plateau (peak 2) into two distinct peaks has been confirmed in low (0.1 at.%) Mn-doped ZnO, it is plausible that the apparent $V_O^\bullet$ level is actually the overlap of Zn_i and V_O levels.

4. Conclusion

ZnO doped with 1/3 mol% Mn_3O_4 and sintered at 1000–1300 °C in air showed distinctive varistor behavior with nonlinear coefficient, α between 6 and 17, but was disappeared in the specimen sintered at 1400 °C. Two activation energies of electron conduction in the pre-breakdown region (i.e. grain boundary region) were measured as 0.37 and 0.71–0.96 eV from J–E–T above 400 K. C–V characteristics tell that doping Mn to pure ZnO forms the double Schottky type barrier in the ZnO grain boundary. The barrier height and donor concentration obtained from C–V plots were about 1.0 V and 2×10^{17} cm^{-3} order, respectively. Two deep bulk trap levels in Mn-doped ZnO were confirmed as 0.13 eV and 0.25–0.32 eV by admittance spectroscopy. The former is thought the attractive coulombic center, and the latter being stemmed from singly charged oxygen vacancy, $V_O^\bullet$, both of which are commonly accepted in ZnO varistors. We think that the redox reaction of Mn_3O_4, i.e. the valence change of Mn on heating and cooling of Mn-doped ZnO plays an important role in the formation of the double Schottky barrier and resultant varistor behavior.

References

[1] F. Greuter, G. Blatter, Electrical properties of grain boundaries in polycrystalline compound semiconductors, Semicond. Sci. Technol. 5 (2) (1990) 111–137.

[2] D.R. Clarke, Varistor ceramics, J. Am. Ceram. Soc. 82 (3) (1999) 485–502.

[3] M. Jakani, G. Campet, J. claverie, D. Fichou, J. Pouliquen, J. Kossanyi, Photoelectrochemical properties of zinc oxide doped with 3d elements, J. Solid State Chem. 56 (3) (1985) 269–277.

[4] H.R. Philipp, L.M. Levinson, High-temperature behavior of ZnO-based ceramic varistors, J. Appl. Phys. 50 (1) (1979) 383–389.

[5] I. Barbariol, S. Roitti, An electroconductometric investigation of Mn_3O_4 and the $Mn_3O_4 \leftrightarrow Mn_2O_3$ transformation, J. Mater. Sci. Lett. 3 (2) (1984) 181–183.

[6] K. Mukae, K. Tsuda, I. Nagasawa, Capacitance-vs.-voltage characteristics of ZnO varistors, J. Appl. Phys. 50 (6) (1979) 4475–4476.